Langmuir

Article

pubs.acs.org/Langmuir

Heating-Enabled Formation of Droplet Interface Bilayers Using *Escherichia coli* Total Lipid Extract

Graham J. Taylor and Stephen A. Sarles*

Department of Mechanical, Aerospace, and Biomedical Engineering, University of Tennessee, Knoxville, Tennessee 37996, United States

Supporting Information

ABSTRACT: Droplet interface bilayers (DIBs) serve as a convenient platform to study interactions between synthetic lipid membranes and proteins. However, a majority of DIBs have been assembled using a single lipid type, diphytanoylphosphatidylcholine (DPhPC). The work described herein establishes a new method to assemble DIBs using total lipid extract from *Escherichia coli* (eTLE); it is found that incubating oil-submerged aqueous droplets containing eTLE liposomes at a temperature above the gel−fluid phase transition temperature (T_g) promotes monolayer self-assembly that does not occur below T_g. Once monolayers are properly assembled via heating, droplets can be directly connected or cooled below T_g and then connected to initiate bilayer formation. This outcome contrasts immediate droplet coalescence observed upon contact between nonheated eTLE-infused droplets. Specific capacitance measurements confirm that the interface between droplets containing eTLE lipids is a lipid bilayer with thickness of 29.6 Å at 25 °C in hexadecane. We observe that bilayers formed from eTLE or DPhPC survive cooling and heating between 25 and 50 °C and demonstrate gigaohm (GΩ) membrane resistances at all temperatures tested. Additionally, we study the insertion of alamethicin peptides into both eTLE and DPhPC membranes to understand how lipid composition, temperature, and membrane phase influence ion channel formation. Like in DPhPC bilayers, alamethicin peptides in eTLE exhibit discrete, voltage-dependent gating characterized by multiple open channel conductance levels, though at significantly lower applied voltages. Cyclic voltammetry measurements of macroscopic channel currents confirm that the voltage-dependent conductance of alamethicin channels in eTLE bilayers occurs at lower voltages than in DPhPC bilayers at equivalent peptide concentrations. This result suggests that eTLE membranes, via composition, fluidity, or the presence of subdomains, offer an environment that enhances alamethicin insertion. For both membrane compositions, increasing temperature reduces the lifetimes of single channel gating events and increases the voltage required to cause an exponential increase in channel current. However, the fact that alamethicin insertion in eTLE exhibits significantly greater sensitivity to temperature changes through its T_g suggests that membrane phase plays an important role in channel formation. These effects are much less severe in DPhPC, where heating from 25 to 50 °C does not induce a phase change. The described technique for heating-assisted monolayer formation permits the use of other high transition temperature lipids in aqueous droplets for DIB formation, thereby increasing the types of lipids that can be considered for assembling model membranes.

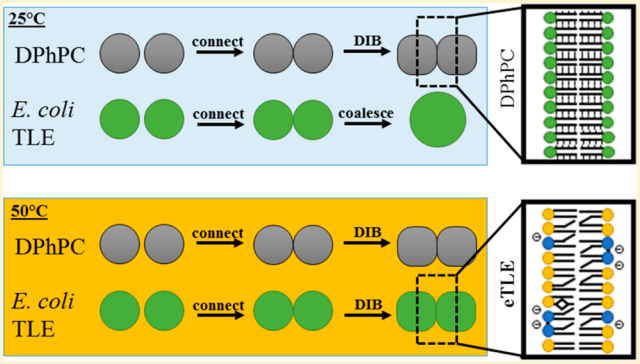

INTRODUCTION

Droplet interface bilayers (DIBs)[1] are gaining momentum as a tool for researching lipid bilayers and membrane-associating proteins from bacterial and eukaryotic organisms.[2−10] Using this platform, a lipid bilayer is formed between two lipid monolayer-encased water droplets submerged in oil. The ability to independently control the contents of each droplet allows symmetric or asymmetric tailoring of the bilayer composition as well as independent tuning of the aqueous solutions on either side of the membrane.[6] As illustrated in Figure 1, studies have utilized DIBs to capture and study membrane-active proteins such as ion-channels, pore-forming peptides,[6,11] and even toxins.[5,8] Demonstrating potential for drug development, DIBs have also been used to monitor the ability of drugs or blocking agents to modulate transmembrane protein behavior.[9,12]

The majority of DIBs have been formed using diphytanoyl phosphocholine (DPhPC), a single lipid type of archeal origin. The reader is referred to the Supporting Information (SI) for a review of lipid selection in published DIB studies. Yet, it is well-known that cell membranes in vivo are comprised of many types of lipids and other molecules (SI, Table S3 for details on natural lipid composition) and that the structures and functions of transmembrane proteins are influenced by membrane

Received: August 29, 2014
Revised: December 15, 2014
Published: December 16, 2014

DOI: 10.1021/la503471m
Langmuir 2015, 31, 325−337

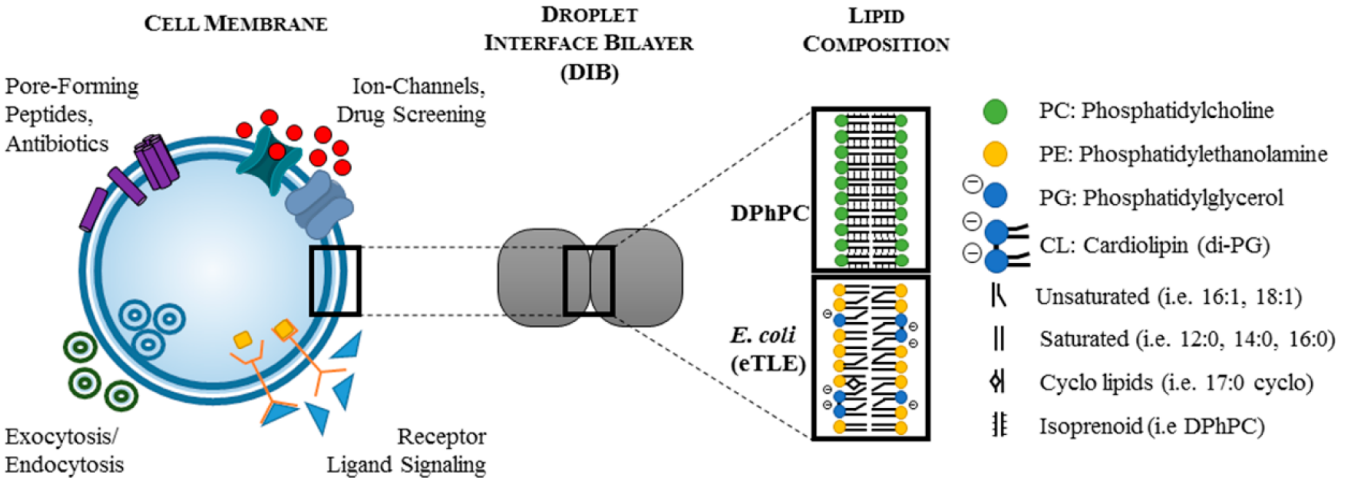

Figure 1. (left) DIBs have been used to create model membranes for studying antimicrobial pore-forming peptides, ion-channels, and drugs or blocking agents interacting with transmembrane proteins. DIBs could potentially be used to study other membrane-mediated processes including receptor-ligand associated signaling, basic vesicle fusion/fission, or higher level trafficking and exo/endocytosis. (right) The majority of DIB research utilizes DPhPC to create single lipid-type bilayers, as shown. A current challenge lies in mimicking the complex composition of natural lipid membranes comprised of multiple lipid types. Total lipid extracts such as the eTLE used herein feature a diverse selection of lipid headgroups and acyl chains, including charged species such as PG and cardiolipin (di-PG).

composition.[13−15] It is also known that many organisms, such as *Escherichia coli* bacteria, actively regulate their lipid compositions in response to environmental conditions like temperature.[16−18] Thus, to be certain that relevant model membranes are available for studying the functions of bacterial and eukaryotic proteins, there is a need for the ability to use complex, naturally occurring lipid mixtures for forming DIBs.

A truly mimetic bacterial model membrane could be used to study the natural functions of antimicrobial peptides. For example, it is known that antibiotic resistance in bacteria is partially enforced through increases in membrane rigidity via alteration of fatty acid content, a response that modulates membrane permeation by alamethicin peptides.[19] These types of changes could be studied in vitro by using total lipids extracted from antibiotic resistant bacteria to form DIBs, which could lead to improved understanding of bacterial resistance and the development of more effective antibiotics. Furthermore, the ability to create DIBs using natural extracts from bacterial or eukaryotic organisms could provide a means to study complex transmembrane proteins such as G protein-coupled receptors (GPCRs) and other proteins with 7 or 12 transmembrane spanning domains.[20,21] Processes such as receptor−ligand-mediated signaling or liposome-mediated trafficking could also be studied in bilayers that mimic the mechanical properties, charge distribution, and fluidity of membranes found in living organisms.[22,23] Until now, however, there is no clearly defined method for forming droplet interface bilayers with total lipid extract obtained from cells.

In contrast to reconstituting cellular membrane fragments into a DIB formed with DPhPC,[4] this work focuses on the assembly and characterization of bilayers from naturally occurring lipid mixtures without the need for added synthetic lipids. Total lipid extract is preferred over assembling model membranes using a mixture of synthetic lipids for two reasons: (1) obtaining a ready-to-use total extract is easier and less subjective than selecting and then carefully mixing synthetic lipids, and (2) it is desired to mimic the full lipid composition of the membrane, including "unknown" components that may play crucial roles in membrane−protein interactions. For example, the "unknown" fraction of brain total lipid extract contains novel membrane lipids and signaling molecules that are vital in neural membrane communication.[24]

Herein, we report that regulated heating allows formation of DIBs using total lipid extract from Gram-negative *E. coli* bacteria. Forming bilayers with *E. coli* total lipid extract (eTLE) is enabled using a recently designed platform for controlled heating of DIBs, and we examine the effects of temperature to determine why heating is required for eTLE DIBs and how temperature affects the bilayer. The eTLE mixture is expected to result in DIBs constructed with a symmetric lipid composition that mimics the inner cytoplasmic membrane of *E. coli* (refer to SI, Table S3). The composition of the inner membrane is largely representative of the total phospholipid composition for total lipids in *E. coli*[18,25] as depicted in Figure 1 (adapted from *E. coli* composition data in Table S3). Phospholipids in *E. coli* are distributed between three main classes in terms of lipid headgroups: neutral phosphatidylethanolamine (PE), negatively charged phosphatidylglycerol (PG), and cardiolipin (CL), which is a PG dimer carrying a double-negative charge. Acyl chains in lipids of *E. coli* consist largely of monounsaturated (UFA), saturated (SFA), or cyclopropane (CFA) fatty acids. As illustrated in Figure 1, the complexity of a bilayer with natural lipid composition is significantly greater than that of a DPhPC-only membrane.

As with prior DIB studies, we show that bilayers formed using eTLE are capable of reconstituting proteins or peptides.[5−8,11] Specifically, we use single channel current recordings, cyclic voltammetry measurements, and circular dichroism to compare the insertion of alamethicin (Alm), a naturally occurring and well-characterized antibiotic peptide produced by *Trichoderma viride* fungus,[26] into eTLE bilayers to that for DPhPC membranes. Single channel recordings are performed at low peptide concentrations, while cyclic voltammetry (CV) is used to examine macroscopic voltage- and temperature-dependent effects of Alm-associated permeation at moderate peptide concentrations in both eTLE and DPhPC DIBs. Circular dichroism (CD) is also used to monitor temperature-dependent changes in the secondary structures of

DOI: 10.1021/la503471m
Langmuir 2015, 31, 325−337

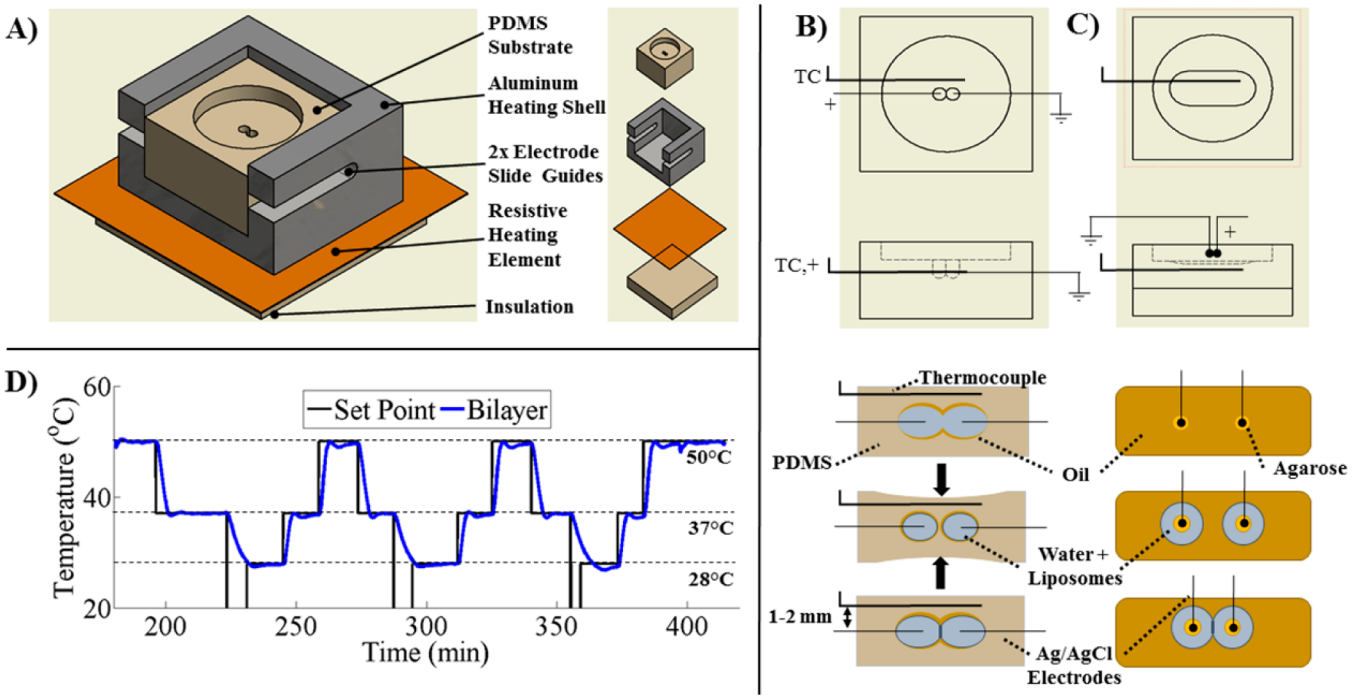

Figure 2. (A) The experimental platform for temperature-controlled heating of DIBs utilizes a PDMS substrate to hold oil and droplets, a resistive heating element, and a heat distributing shell assembled as shown. (B,C) Top and front views of two types of PDMS substrates used for DIB formation (B) via the regulated attachment method or (C) between suspended droplets on movable electrodes. The outer geometry of both substrates is identical, and the thermocouple (TC) is inserted into the same location within both PDMS substrates (refer to the text for more details). (D) Representative measurements of temperature tracking within the substrate using on−off, PI feedback temperature control.

peptides incubated at high concentration with eTLE and DPhPC liposomes.

MATERIALS AND METHODS

Materials. Aqueous buffer is prepared by titrating a 100 mM sodium chloride (NaCl, Sigma), 10 mM 3-(*N*-morpholino)-propanesulfonic acid (MOPS, Sigma) stock solution with an identical solution supplemented with 0.5 M sodium hydroxide (NaOH, Sigma) to achieve pH 7.4 as measured using an Accumet AP85 pH probe (Fisher Scientific). 1,2-Dimyristoyl-*sn*-glycero-3-phosphocholine (DMPC), 1,2-diphytanoyl-*sn*-glycero-3-phosphocholine (DPhPC), *E. coli* total lipid extract (eTLE), and 1,2-dipalmitoyl-*sn*-glycero-3-phosphocholine (DPPC) lipids are acquired as lyophilized powders from Avanti Polar Lipids, Inc. and separately dissolved into aqueous buffer before being subjected to five freeze/thaw cycles to create stock solutions of multilamellar liposomes. Unilamellar DPhPC and eTLE liposomes are created by extruding the thawed stock lipid solutions through 100 nm pore polycarbonate membranes (Whatman) using an Avanti Mini Extruder. DPPC liposomes are created via 5−7 h of sonication at 55 °C in a bath sonicator[27] (FS20D, Fisher Scientific). Final liposome solution concentrations are 2 mg/mL for DIB, CD, and DSC measurements. DPhPC and eTLE liposome solutions are stored at 4 °C, while DPPC liposome solutions are stored at room temperature. Hexadecane (99%, Sigma) is used for the oil phase in all DIB testing. Alamethicin peptides (A.G. Scientific) from *T. viride* are dissolved in ethanol (Sigma) at 10 mg/mL and diluted with aqueous buffer to a final concentration of 2.5 mg/mL to create a stock solution that is stored at −20 °C. For DIB testing with Alm, the frozen peptide stock is thawed and diluted to 25 μg/mL (0.25% ethanol remaining) with buffer before adding it to 2 mg/mL unilamellar liposomes to achieve the desired final Alm concentration. This approach minimizes dilution of the liposomes while ensuring adequate dilution of the original ethanol solvent. Separately, alamethicin stock and liposome solutions are diluted and combined to create samples with 500 μg/mL lipid and 50 μg/mL Alm (peptide/lipid ratio ∼ 1:46) for CD. Peptide/lipid stock solutions are stored at 4 °C and used within 2 weeks.

Differential Scanning Calorimetry (DSC). Aqueous liposome solutions are first placed under vacuum for 10 min to remove air bubbles. Then, 15 μL of liposome solution is loaded into standard hermetic pans (TA Instruments) that are sealed using a Tzero Press (TA Instruments). Measurements are performed with a Q2000 differential scanning calorimeter (TA Instruments) via the following protocol: (1) temperature reduced and held at 10 °C for 5 min, (2) temperature increased at a rate of 5 °C/min to 80 °C, (3) temperature decreased to 10 °C, and (4) repeat steps (1)−(3) three more times. The first cycle is performed to erase thermal history. Unilamellar liposome suspensions are preferred over multilamellar suspensions which show transience in enthalpies with repeated scans.[28] Identical measurements are performed using plain buffer solution as a reference sample for subtraction from calorimetric scans of liposome suspensions to resolve the signal resulting from liposomes alone.

Feedback-Controlled Heating of DIBs. Figure 2A shows an isometric view of the heating platform including the polydimethylsiloxane (PDMS) regulated attachment (RAM) substrate used for regulating droplet attachment as described previously (Figure S4 shows a full setup).[7] The RAM substrate (Figure 2A,B) is used in all DIB experiments except for those in which submerged droplets suspended on agarose-coated electrodes are used for measuring specific bilayer capacitance. Typical droplet sizes for RAM and suspended droplet tests are 700 and 300 nL, respectively. The PDMS substrate is placed within an aluminum shell that rests on top of a 30 mm × 30 mm resistive polyimide flexible heating element (Omega, KHLV-101/10). An insulating PDMS wafer is placed beneath the heater to reduce heat loss in the downward direction. The four-wall design of the heating shell preserves access to one side of the substrate for lateral compression during bilayer formation,[7] while the shell itself allows for faster, more even heating of the PDMS substrate. A silver−silver chloride (Ag/AgCl) electrode made from 120 μm diameter silver wire soaked in bleach is inserted through the substrate into each compartment. A thermocouple inserted into the PDMS substrate

DOI: 10.1021/la503471m
Langmuir 2015, 31, 325−337

measures temperature near the bilayer region. The 152 mm long, 2.4 mm diameter steel-encased thermocouple probe (Omega P/N JMTSS-020U-6) allows direct insertion and fixation within the flexible substrate. When placed parallel to the electrodes at a distance <2 mm from the droplet compartments, the thermocouple records temperature within 1 °C (+1/−0 °C) of the temperature of the bilayer region (confirmed in separate tests) without directly interfering with the droplets or bilayer. Temperature is recorded using a custom LabVIEW Virtual Instrument (VI) in communication with a National Instruments (NI) four-channel thermocouple input module (NI 9211) within a NI CompactDAQ (cDAQ-9174). On−off, proportional-integral (PI) feedback temperature control is implemented within the same VI to enable controlled heating and passive cooling of the bilayer temperature to within +/−0.3 °C of a desired value. Figure 2D shows the bilayer region temperature and system response to discrete changes (via the VI) in the desired temperature (set point).

DIB Electrical Measurements. Current measurements on DIBs are made using an Axopatch 200B patch clamp amplifier and Digidata 1440 data acquisition system (Molecular Devices). All recordings are made within a grounded Faraday cage where RMS noise is less than ±3 pA. Voltage waveforms generated by a custom LabVIEW VI and NI 4-channel analog output module (NI 9263) are routed to the headstage via the external command input on the amplifier. Waveforms used in this study include (1) a 10 mV, 10 Hz triangular voltage waveform to measure bilayer capacitance, (2) an automated DC voltage step routine to measure bilayer resistance and rupture potential, and (3) CV scans to determine the voltage threshold of Alm−DIB interactions. Additional information is provided in the SI (Figures S1−S3).

DIB Specific Capacitance Measurements. The specific membrane capacitance (C_M) is measured for DIBs formed between droplets suspended on electrodes (Figure 2C) using a method similar to that reported elsewhere.[29] These experiments require simulataneous measurement of both the nominal capacitance and the area of the bilayer (contact area between droplets). Nominal bilayer capacitance (C_T) is determined via the measured current induced by a triangular waveform voltage, while area is computed from a measurement of bilayer diameter determined from an image of the connected droplet pair. Values of steady-state capacitance and bilayer area are recorded for varying amounts of contact between droplets by manually manipulating the electrode positions. DIB images are analyzed via an automated image processing routine to consistently determine bilayer diameter and compute bilayer area (A_M). Additional details of this method can be found in the SI.

Circular Dichroism (CD) Spectroscopy. CD spectroscopy is performed in 1 mm path length quartz cells with a Jasco J-810 CD spectropolarimeter. For both eTLE and DPhPC liposomes, solutions are created with a lipid/peptide (L:P) ratio of approximately 1:46 using stock solutions described above. Scans are performed first at 25 °C for each lipid type before heating to 37 and 50 °C. Cuvette and sample temperature are maintained using a Jasco temperature controller (JWJTC-484), with at least 5 min provided for temperature equilibration prior to sample measurement. Data are collected at standard resolution (±100 millidegrees) every 0.5 nm from 190 to 300 nm with a scan rate of 50 nm/min and response time of 2 s. Five scans are averaged to produce the final spectra. Scans conducted using buffer and lipids alone (no Alm) provide background signal to be removed from data obtained including Alm. To minimize the effects of drift in measurements, spectra are corrected by removal of any nonzero ellipticity measured at 260 nm where the signal should otherwise be zero.[30]

RESULTS AND DISCUSSION

Bilayer Formation Using eTLE. Attempts to form DIBs using lipids extracted from *E. coli* were guided by two facts: (1) membranes of living organisms display thermotropic phases,[16−18,31] and (2) lipid monolayer assembly at a polar−nonpolar liquid−liquid interface is affected by temperature-dependent phase transitions of liposomes.[32] DSC is first used to identify transition temperatures in liposomes made from *E. coli* total lipid extract, as well as DPhPC and DPPC synthetic phospholipids. DPPC lipids are included as a reference since they are known to undergo a gel-to-liquid phase transition at a temperature of 41−43 °C. The resulting thermograms for eTLE, DPhPC, and DPPC are provided in Figure 3. As

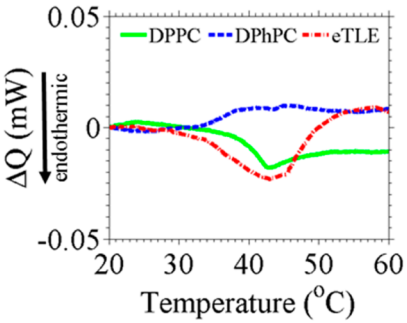

Figure 3. Differential scanning calorimetry (DSC) thermograms obtained from heating aqueous unilamellar liposomes of DPPC, DPhPC, and eTLE between 10 and 80 °C at a rate of 5 °C/min. Data is presented as change in heat (ΔQ). Downward deflections indicate endothermic heat absorption.

expected, the negative change in heat measured by the instrument near 42 °C confirms that DPPC liposomes undergo an endothermic melting transition from gel to fluid phase. DPhPC, a lipid expected to exist in a single gel phase between −120 and 120 °C,[33] does not exhibit a similar melting transition upon heating from 20 to 60 °C. In contrast, eTLE displays a broad endothermic transition centered about 44 °C. This result suggests that heterogeneous eTLE bilayers undergo a gel-to-fluid melting transition when heated from 40 to 50 °C. The center of this endothermic range is in agreement with a reported transition at 41−43 °C that was observed in fluorescence anisotropy and DLS experiments with eTLE.[34]

The DSC results provide knowledge about the temperature-dependence of eTLE bilayers in an aqueous environment. However, the goal of this research is to form DIBs using eTLE lipids, which first requires liposomes present inside the droplets to facilitate the assembly of a well-packed lipid monolayer at the oil-water interface. Therefore, a series of experiments was performed to test DIB formation between two droplets containing eTLE liposomes in hexadecane (Figure S6). Similar trials using DPhPC are included for comparison. Both the time allowed for monolayer formation (t_m) at the droplet surfaces and the temperature of the liquid environment were varied. Droplets are introduced separately into the adjacent compartments of the RAM substrate at $t_m = 0$, and the volumes are kept apart by compressing the flexible substrate. Current measurements are used to monitor bilayer formation upon initiating droplet contact. Highly resistive lipid bilayers produce a stable, square current waveform, leaky membranes yield an ohmic triangular current response, and coalesced droplets yield a saturated current in response to the continuously applied triangular voltage waveform (examples of the current response for each state are provided in Figure S6A,B in the SI).

The general results from this experiment are illustrated in Figure 4. While DPhPC DIBs form after 3−5 min (Figure S6F) of droplet incubation in oil at room temperature, we found that droplets containing eTLE liposomes do not form a DIB at room temperature. Instead, eTLE-doped droplets coalesce upon contact, even in tests allowing up to 1 h of incubation

DOI: 10.1021/la503471m
Langmuir 2015, 31, 325−337

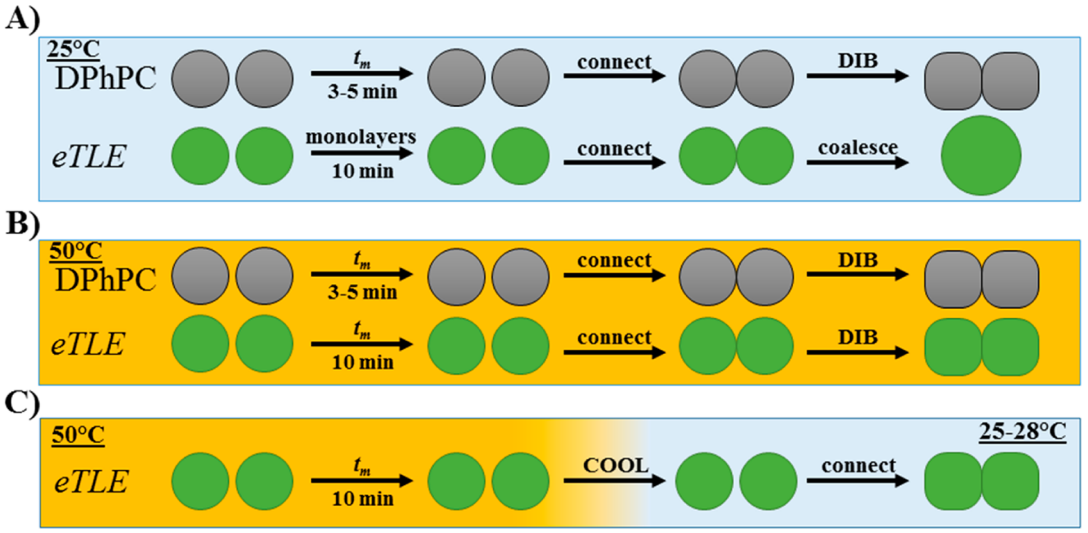

Figure 4. Approaches taken to attempt bilayer formation in hexadecane using aqueous droplets containing 2 mg/mL DPhPC or eTLE lipids: (A) At 25 °C, DPhPC droplets resist coalescing when connected after only 3−5 min for monolayer assembly. In contrast, eTLE droplets coalesce at room temperature even after 1 h for monolayer assembly. (B) With the system (oil, substrate, and droplets) heated to 50 °C, droplets containing DPhPC enable bilayer formation after 3−5 min for monolayer assembly, and eTLE droplets allow bilayer formation after 10 min for monolayer assembly. (C) eTLE droplets can be introduced at 50 °C with 10 min for monolayer assembly before cooling the entire system to room temperature and then connecting the droplets. In contrast to coalescence as observed in (A), eTLE droplets allow for DIB formation at room temperature via this treatment, confirming that heating to a temperature above T_g promotes self-assembly of lipid monolayers.

time for monolayer formation (Figure 4A, Figure S6C). This result indicates that a well-packed lipid monolayer does not assemble at the droplet surfaces at room temperature with eTLE liposomes. The oil temperature was then gradually increased to determine if monolayer assembly and DIB formation could instead occur at an elevated temperature. The current recordings (Figure S6D) demonstrate that not until the temperature reached 50 °C did we observe two droplets containing *E. coli* liposomes form a stable interface bilayer as indicated by a square current response. Additional trials at this temperature were performed to determine that an incubation time of 10 min at 50 °C allows for consistent DIB formation with eTLE (Figure 4B, S6E). We confirmed that droplet diameter remains unchanged over the course of an hour at 50 °C to rule out the possibility of evaporation induced monolayer assembly and packing.

A final series of DIB formation tests was performed at room temperature (25 °C) after a 10 min incubation period at 50 °C (illustrated in Figure 4C) to determine if heating is required for both monolayer assembly and bilayer formation. Like those that were incubated and connected at 50 °C, we found that eTLE DIBs readily form after cooling to room temperature following incubation at 50 °C. These results suggest that (1) heating above T_g enables improved monolayer assembly at the oil−water interface from fluid-phase liposomes, which more readily assemble to reduce surface tension;[32] and (2) that DIBs can be formed with lipids in the gel phase, so long as the opposing lipid monolayers are well-packed.

To test this idea, we attempted DIB formation with two types of saturated synthetic lipids, DMPC (T_g = 25 °C) and DPPC (T_g = 41-43 °C), which display transition temperatures above room temperature. To our knowledge, these lipid types have not been incorporated as liposomes into droplets to form DIBs. Instead, previous attempts to form DMPC or DPPC bilayers between water droplets incorporated lipids into the organic phase,[35−38] where the phase behavior of inverse lipid micelles in oil may not correlate to that for bilayers in an aqueous environment. In numerous trials at room temperature, DMPC or DPPC liposome-infused droplets coalesce (100% failure rate) when brought into contact. Coalescence is encountered even in tests allowing 30 min or more for monolayer formation, much like droplets containing eTLE at room temperature described above. A long-lasting lipid bilayer can be assembled by heating DMPC droplets to 35−45 °C and DPPC droplets to 50−60 °C (SI, Figure S7) for 10 min before bringing droplets together. However, unlike eTLE DIBs, we observe these single component membranes to rupture when cooled through T_g, a result that has been reported by others.[40,41]

The combined result from DIB formation and DSC measurements is that monolayer assembly and thus bilayer formation improves drastically when the mixed lipids are heated above their effective T_g. This finding is in close agreement with Lee and Needham's study of homogeneous monolayer assembly using saturated phosphatidylcholine lipids supplied to the interface as liposomes, which showed that maximum monolayer surface pressure is reached only when the system temperature is above T_g.[32] What our results add is that the phase behavior of the liposomes is an important factor in DIB formation for lipids with transition temperatures above room temperature and that in situ heating control can be used to enable monolayer formation for lipids with high transition temperatures.

Specific Capacitance versus Lipid Composition and Temperature. Measurements of capacitance per unit area are used to confirm that the interface between noncoalescing droplets containing eTLE is a bilayer. Specific capacitance of DPhPC bilayers assembled from liposomes in the droplets is also measured. C_M is determined for bilayers assembled from each lipid type at 25, 37, and 50 °C, and the results from these measurements are provided in Figure 5A. At 25 °C, we find C_M to be 0.74 ± 0.022 μF/cm^2 for DPhPC DIBs, a value that is in close agreement with previously reported values of 0.65 ± 0.2 μF/cm^2[39] and 0.64 ± 0.003 μF/cm^2[29] for DIBs formed using

DOI: 10.1021/la503471m
Langmuir 2015, 31, 325−337

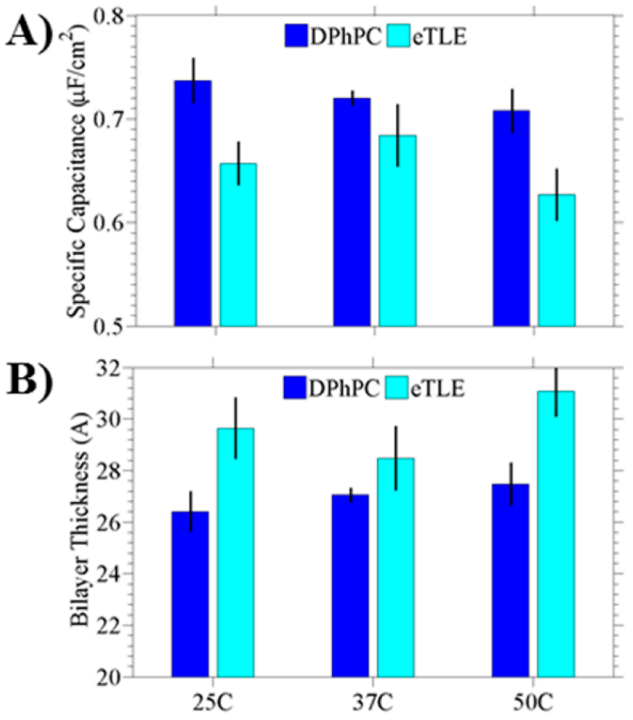

Figure 5. (A) Specific capacitance (C_M) and (B) hydrophobic region thickness (d_M) of eTLE and DPhPC bilayers formed at 25, 37, and 50 °C. Bars represent the average values for each case with lines showing ±1 standard deviation. Actual values, including standard deviation and number of trials for each case, are included in Table S4 in SI.

DPhPC in hexadecane. The measured C_M value of 0.66 ± 0.021 μF/cm^2 for eTLE DIBs at 25 °C shows that the capacitance per unit membrane area of these interfaces is close to that for DPhPC DIBs.[29] Measurements at 37 and 50 °C yield similar values of C_M for both membranes. Yet, while DPhPC exhibits a consistent decrease in specific capacitance with rising temperature, eTLE membranes exhibit a peak specific capacitance of ca. 0.68 μF/cm^2 at 37 °C, before falling back to ca. 0.62 μF/cm^2 at 50 °C. Given that synthetic lipid bilayers are known to exhibit specific capacitances between 0.5 and 1.0 μF/cm^2,[42] these data provide strong evidence that the interface formed between noncoalescing eTLE-doped droplets is that of a thinned lipid bilayer,[3] regardless of the temperature at which the membrane forms.

The specific capacitance of a bilayer is related to the thickness of the hydrophobic bilayer interior (d_M) as given by $C_M = \varepsilon\varepsilon_0/d_M$, where ε and ε_0 are the dielectric coefficient of the hydrophobic region and the permittivity of free space, respectively. Hydrophobic thicknesses for eTLE and DPhPC bilayers (Figure 5B) formed across the range of 25−50 °C are estimated using the measured values of C_M and a value of 2.2 for the dielectric coefficient.[43,44] These data reveal that the hydrophobic thickness of a DPhPC bilayer is approximately 26 Å at 25 °C, whereas an eTLE membrane at the same temperature has a hydrophobic thickness closer to 30 Å. This comparison suggests that eTLE membranes are nearly 12% thicker than DPhPC bilayers at 25 °C, despite the fact that both membranes contain large fractions of 16-carbon acyl chains (refer to SI, Table S3) and are expected to have a similar dielectric constant. Estimates of thickness at elevated temperatures show that the thickness of the membrane is sensitive to temperature. DPhPC membranes steadily thicken, from 26.4 to 27.5 Å, as the droplets are heated from 25 to 50 °C, while eTLE exhibit thicknesses ranging from 28.4 to 31.0 Å.

The temperature dependence of membrane capacitance and thickness for a synthetic lipid bilayer depends greatly on the presence and amount of trapped hydrocarbon solvent in the membrane. In cases where a membrane is completely *solvent-free*, experiments and theory confirm that the thickness of a solvent-free membrane increases upon cooling.[45,46] At temperatures above the gel−liquid phase transition for the membrane, the membrane is relatively thinner due to a reduced length and higher area per lipid in the bilayer. The lipids elongate and the area per lipid reduces as it cools from the more-disordered liquid state to the more-packed gel state. These types of thickness changes relative to the T_g have been observed via atomic force microscopy[45] or small angle neutron scattering/X-ray scattering data[46,47] on solvent-free bilayers, where one would expect a lower C_M in the gel phase as a result. However, the dependence of membrane capacitance and thickness on temperature has been shown to be opposite for synthetic lipid bilayers in which equilibrium between the thinned bilayer region and the surrounding annulus results in oil trapped in the membrane. In the *solvent-containing case*, increasing the temperature results in changes to the lipid phase that are consistent with those for a solvent-free membrane, but also changes in the net amount of oil in the bilayer (the entropic penalty for excluding oil decreases with higher temperature leading to more solvent in the membrane).[48] As a result, a shortening of the lipid lengths as the membrane is heated from the gel-to-liquid phase is counteracted by an increase in the amount of oil trapped in the bilayer. White showed that the net effect is a thickening of the bilayer, as shown by a decrease in specific capacitance, with increasing temperature.[48]

Our results on eTLE bilayers using hexadecane, which is known to remain in DPhPC bilayers,[29] show a temperature-dependence for membrane capacitance that agrees in both magnitude and direction with White's results[48] on suspended planar bilayers in the presence of alkane solvents. The fact that we do not observe an increase in C_M upon heating eTLE through the phase transition indicates that the membrane is not completely *solvent-free*. Conversely, the subtle decrease in C_M upon heating denotes a slight increase in the oil fraction in the bilayer. While DPhPC bilayers have been shown to contain ca. 10% hexadecane by volume,[29] it is unknown from our data alone how much the thickness of an eTLE membrane corresponds to solvent. Follow up measurements on solvent-free eTLE membranes achieved with a different oil are required to estimate the hydrophobic thickness of the mixed-lipid membrane. Interestingly, the higher value of C_M measured at 37 °C, which aligns well with the phase transition region for eTLE bilayers (Figure 3), may indicate that oil is excluded to a greater degree near the phase transition. However, this result is not conclusive with few measurements of C_M at widely spaced values of temperature.

Effects of Temperature on Bilayer Electrical Properties. A high electrical resistance (>1GΩ) is important in synthetic lipid bilayers because it shows that the membrane creates an effective seal between the two aqueous phases, which minimizes unwanted diffusion of species and reduces leakage current in single channel measurements of transmembrane proteins.[4,5] Measuring the voltage-induced rupture potential provides an idea of the practical range of voltages that can be applied to study membranes and membrane-associating proteins.[4,5] Rupture potential tests also provide information

DOI: 10.1021/la503471m
Langmuir 2015, 31, 325−337

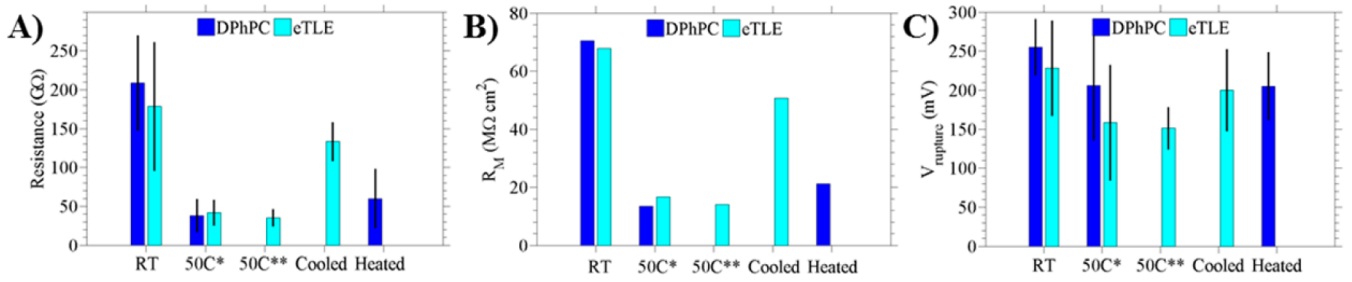

Figure 6. (A) Nominal bilayer resistance, (B) membrane resistance (resistance × area), and (C) rupture potential obtained for the various combinations of lipid type and temperature tested herein. Bars represent the average values for each case, with lines showing ±1 standard deviation. Actual values, including standard deviation and the number of trials for each case, are included in Table S4 in the SI. For (B), resistance is taken from (A), while area is computed based on a bilayer capacitance of 250 pF established in all tests and an appropriate value of C_M as determined above (Figure 5) for each lipid/temperature combination. *t_m = 10 min. **t_m = 30 min.

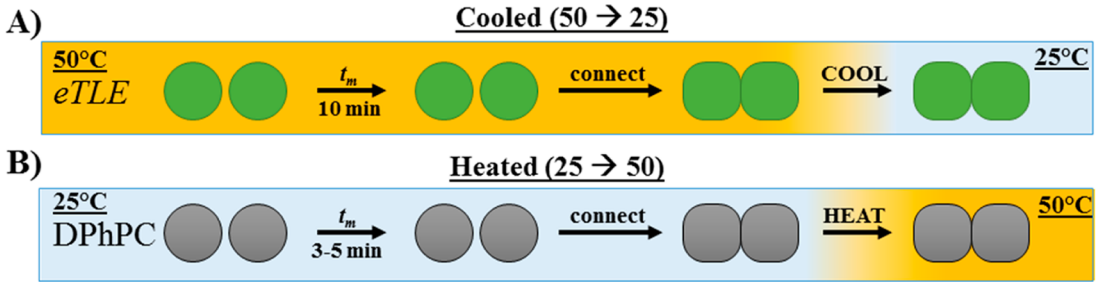

Figure 7. (A) Approach for forming an eTLE DIB at 50 °C before cooling it to room temperature. (B) Similarly, the approach to assemble a DPhPC DIB at room temperature followed by heating to 50 °C. Refer to the text for descriptions of test results and electrical properties of heated/cooled DIBs.

regarding membrane sensitivity to electroporation and lipid ion-channel formation.[49] Thus, in addition to specific capacitance measurements described above, experiments are performed to characterize the electrical resistance and rupture potential of both eTLE and DPhPC membranes at two bilayer formation temperatures: room temperature (25 °C) and 50 °C.

In these tests, eTLE DIBs are formed at either 25 or 50 °C between droplets incubated for 10 min in oil at 50 °C, while DPhPC DIBs are formed at either temperature after 3−5 min for monolayer formation. Membrane resistance and rupture potential are extracted from current measurements obtained using the DC step voltage routine described in Materials and Methods (a full description of resistance and rupture potential experiments is also provided in the SI). Figure 6 provides a summary of measured resistance, specific resistance, and rupture potential measured for eTLE and DPhPC DIBs formed at both temperatures. At 25 °C, eTLE and DPhPC DIBs exhibit statistically similar nominal (Figure 6A) and specific resistances (Figure 6B) on the order of 100 GΩ and 70 MΩ·cm^2, respectively. These levels of resistance are consistent with values reported for other DIBs[4,5] tested at room temperature. The data also reveal that both eTLE and DPhPC bilayers formed at 50 °C exhibit lower values of resistance; specific resistance for both drops from approximately 70 MΩ·cm^2 to <20 MΩ·cm^2. Independent-sample t tests confirm that for each lipid type bilayer resistance is significantly lower (i.e., $p < 0.05$) at 50 °C versus 25 °C. This result suggests that bilayer conductivity, and thus permeability to ions, increases with temperature with bilayers of DPhPC and eTLE as well. Nonetheless, both membrane compositions exhibit nominal resistances greater than 20 GΩ across the temperature range tested (25−50 °C) and neither exhibit leakage currents in response to an applied voltage. Similar to resistance, the data in Figure 6C show that eTLE and DPhPC exhibit similar values of rupture potential, and that rupture tends to occur at a lower voltage for DIBs assembled and tested at 50 °C. More specifically, rupture potentials are found to be greater than 150 mV for all lipid and temperature combinations, even though there is no significant difference in rupture potential as a function of temperature ($p > 0.05$) for either lipid type.

Given reports of droplet coalescence during heating of DIBs,[36,40,50] we are also motivated to determine if the bilayer can withstand a dynamic change in temperature and understand how this change in condition affects bilayer resistance and rupture potential. Thus, a group of tests is conducted to examine the effects of dynamically cooling an eTLE DIB formed at 50 °C as illustrated in Figure 7A (additional data in the SI, Figure S10A). To do so, the system temperature set point is changed to 25 °C after DIB formation to allow the bilayer and adjoining droplets to passively cool from 50 to <28 °C in about 15 min, at a maximum cooling rate of 3−4 °C/min (Figure S10F). We found that eTLE bilayers were able to withstand the decrease in temperature without rupturing in 11 of 11 separate cooling trials. Nominal resistance, specific resistance, and rupture potential measured for the "cooled" eTLE DIBs after cooling to room temperature are provided in Figure 6.

Conversely, we examine the effects of increasing temperature on DPhPC bilayers formed at room temperature by controllably heating them to 50 °C (Figure7B, S10G). Similar to eTLE DIBs, heated DPhPC bilayers remain intact (in 9 of 9 trials) during the temperature change, even with heating rates greater than 10 °C/min (Figure S10L). The active heating provided by the temperature controller is responsible for the increased rate of temperature change with heating compared to cooling, achieving the prescribed increase from room temper-

DOI: 10.1021/la503471m
Langmuir 2015, 31, 325−337

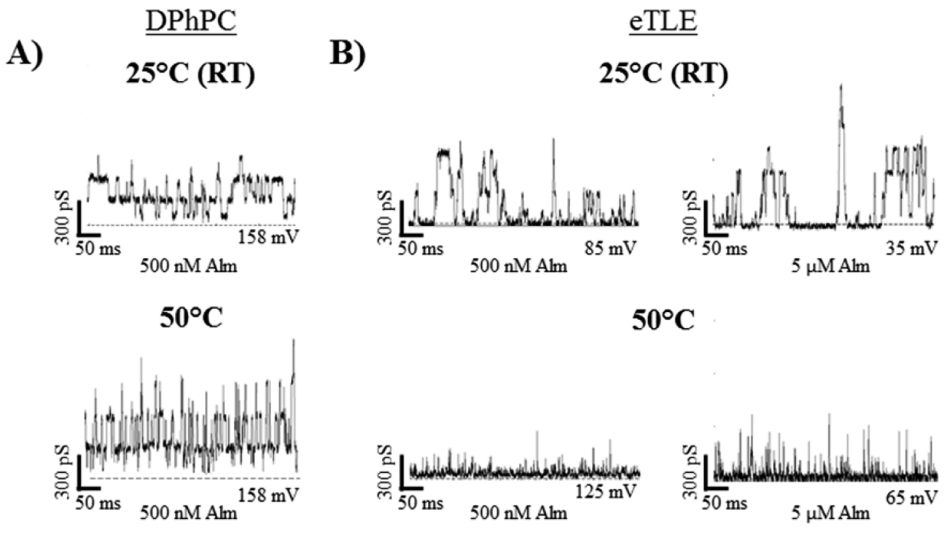

C)

	DPhPC	*E. Coli* TLE	
Alm Conc.	500nM	500nM	5uM
Level	G (pS)	G (pS)	G (pS)
0	0.0	0.0	0.0
1	18.3	17.3	-
2	78.8	87.8	90.5
3	226.1	252.1	266.9
4	398.8	437.1	463.0
5	606.0	570.49	615.7

Measured at 25°C

Figure 8. Single channel alamethicin (Alm) gating with (A) DPhPC and (B) eTLE DIBs incorporating Alm in the *cis* (+electrode) droplet. Concentrations tested include 500 nM and 5 μM, and tests are performed at 25 and 50 °C which is below and above, respectively, T_g for the eTLE lipid mixture. The applied voltage is indicated with each trace. (C) Single-channel conductance levels for DPhPC and eTLE bilayers at 25 °C, computed from multiple gating events (all data not shown) at different Alm concentrations.

ature to 50 °C in just a few minutes. Values for the electrical properties of "heated" DPhPC DIBs formed at room temperature and warmed to 50 °C are shown in Figure 6 (see Table S4 also). Like those formed and tested at 50 °C, DPhPC membranes heated to 50 °C after assembly at 25 °C exhibit statistically lower values of resistance than is measured for DPhPC membranes formed and tested at room temperature.

These findings prove that DIBs formed from DPhPC or eTLE can withstand temperature changes without rupturing. Yanagisawa et al.[36] reported that DIBs made from saturated dimyristoyl or dipalmitoyl phosphocholine (DMPC or DPPC) lipids (incorporated as inverse micelles into the organic phase) rupture during heating from 20 to 50 °C. Dixit et al. (DPhPC liposome solution),[50] and Villar et al. (a 3:1 DSPC:DPhPC mixture in oil)[40] also separately observed droplet coalescence and bilayer rupture while heating intradroplet bilayers, with the latter at a heating rate of only 1 °C/min. We report here that DIBs made from both eTLE and DPhPC phospholipids incorporated as liposomes within the droplets remain intact while heating between 20 and 50 °C at rates as high as 10−11 °C/min. The key difference here is that DIBs are formed from either a complex mixture of lipids (eTLE) or lipids that do not undergo a phase transition (DPhPC). Single-component membranes are known to exhibit increased permeability and inherent stability near the phase transition due to having a sharp maximum in heat capacity at the transition.[49] As a result, bilayers formed from single lipids and binary mixtures are inherently weak and rupture easily upon cooling through T_g. The cited reports showing rupture near T_g with DMPC, DPPC, and DSPC:DPhPC bilayers are good examples of this outcome. In contrast, membranes consisting of many lipid types exhibit broader transitions with lower susceptibility to rupture. The fact that eTLE survives heating and cooling through its T_g is attributed to its diverse lipid profile that preserves fluidity and a low permeability through the transition. On the other hand, our DPhPC DIBs are believed to survive for the reason that they do not pass through a transition in the temperature range tested. While this finding contrasts a prior study showing DPhPC failure,[50] we note that the authors of that work induced localized heating via an infrared laser and temperature and heating rate were not measured or controlled.

Lipid Composition Influences Peptide−Membrane Interactions. Having a reliable method to construct lipid bilayers from *E. coli* total lipid extract enables the study of interactions between transmembrane proteins and bilayers possessing natural and heterogeneous lipid composition. A series of experiments are performed to determine how the insertion of alamethicin (Alm), a well-characterized antimicrobial peptide, differs between eTLE and DPhPC DIBs. First, it is necessary to ensure that no channel-like activity exists in eTLE DIBs formed in the absence of Alm. This control is especially important considering that almost 20% of the mixture is "unknown" (Avanti). In control tests without Alm, we observe no channel-like currents across a wide range of applied voltages and bilayer lifetimes. Even large eTLE bilayers exhibit no transient current with voltage clamped for several minutes at 150 mV (Figure S11). Control tests with DPhPC also result in quiet baselines at voltages below the rupture potential. In contrast, the addition of Alm to the *cis* droplet (+electrode) of either DPhPC or eTLE DIBs introduces significant voltage-dependent changes in membrane conductance, giving rise to either microscopic single-channel or macroscopic aggregate-channel currents depending on Alm concentration.

Figure 8A and B shows representative alamethicin activity measured at room temperature (25 °C) in both DPhPC and eTLE DIBs with 500 nM Alm in the *cis* droplet. In bilayers of either lipid type, the current (conductance) signal stochastically fluctuates between discrete levels signifying single channel pore formation, as previously established.[51,52] Yet, voltage-dependent gating events occur at much lower voltages for eTLE bilayers. For example, Figure 8A shows gating with DPhPC held near 160 mV. In this test, voltages < 160 mV induce little to no activity, while voltages > 160 mV lead to higher currents via the insertion of additional channels. In contrast, measurements of alamethicin gating in eTLE DIBs at 25 °C show single-channel activity near 85 mV (Figure 8B), roughly half of the potential required to promote gating with DPhPC under the same

DOI: 10.1021/la503471m
Langmuir 2015, 31, 325−337

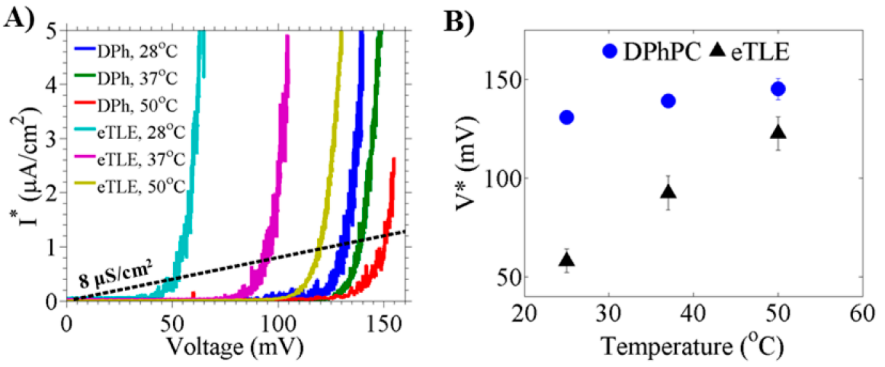

C)

	DPhPC		*E. coli* TLE	
Temp. Group	V* (mV)	ΔV* (mV)	V* (mV)	ΔV* (mV)
RT	130.7 (2.104) *n*=8	0	58.0 (5.931) *n*=6	0
37°C	139.0 *n*=1	+8.3	92.4 (8.561) *n*=7	+34.4
50°C	145.1 (5.360) *n*=7	+14.4	122.6 (8.470) *n*=9	+64.6

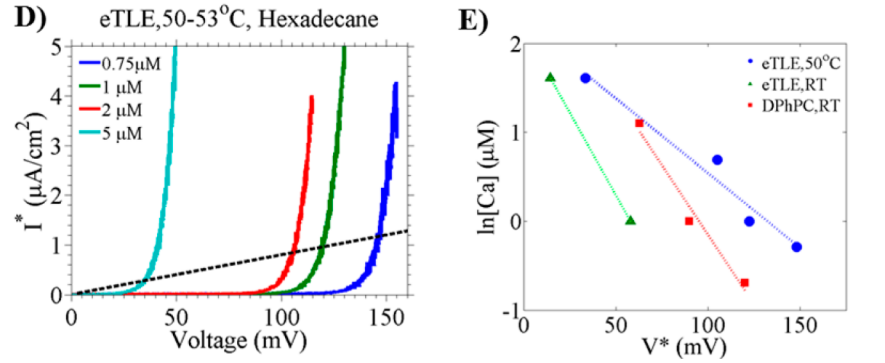

F)

Lipid/ Temp.	**V_a (mV)**	**C_0 (μM)**
DPhPC, RT	31.95	19.72
eTLE RT	26.95	8.59
eTLE, 50°C	59.52	9.24

Figure 9. (A) Specific current (I^*, normalized by membrane area) from one of 10 repeated scans during CV testing at varying temperatures with either DPhPC or eTLE DIBs. The trace shown is an average of I^* recorded during the increasing and decreasing portions of a single scan, resulting in a single I^* signal associated with the linear voltage ramp from 0 to 150 mV. In these tests, the *cis* (+) droplet contains 1 μM alamethicin (Alm). For each lipid case shown, a bilayer is formed at 50 °C, tested via CV, cooled to 37 °C, tested via CV again, and then finally cooled to 28 °C before a third and final round of CV scans. The dashed line represents the conductance threshold (G^*_{thresh}) used to determine voltage threshold (V^*): the voltage at which I^* exceeds G^*_{thresh}. (B) V^* as a function of temperature from part (A). Error bars show ±1 standard deviation (σ). (C) Summary of cyclic voltammetry (CV) testing, including V^* and relative change in voltage threshold (ΔV^*) versus temperature. The value in parentheses is σ. (D) Current−voltage sweeps for an eTLE DIB above T_g with 0.75, 1, 2, and 5 μM Alm. (E) Plot of the logarithmic relationship between V^* and alamethicin concentration, C_a, used to compute the conductance parameters V_a and C_0 shown in (F).

conditions. In separate tests of eTLE DIBs with 5 μM Alm incorporated into the droplet, single-channel events are observed at voltages between 30 and 40 mV. This trend agrees with prior reports[52] of the concentration-dependence of Alm, where increasing peptide concentration reduces the voltage required to attain insertion. The first five unit conductance levels (including the subconductance level at 15−20 pS) for Alm with each lipid type at 25 °C are determined from histograms of many single channel events (representative data in SI Figure S11) and summarized in Figure 8C. The ratios of alamethicin conductance levels relative to the subconductance level in DPhPC bilayers are found to be 1, 4.3, 12.2, 21.6, and 32.8, and for eTLE we obtain ratios of 1, 5.1, 14.6, 25.3, and 33.0. These values for both lipid types compare well with previously reported values,[53] and there appear to be no significant differences in the conductance states between lipid types or for different measurement temperatures, which is consistent with prior findings regarding the effects of membrane composition on Alm conductance levels.[53]

The lower panels of Figure 8A and B show the results of single channel recordings in DPhPC and eTLE DIBs at 50 °C. Discrete stepwise changes in current at the same conductance levels are again observed with DPhPC DIBs at the same voltage shown for room temperature (158 mV). However, these transitions occur at a noticeably higher frequency, a result that is in agreement with previous reports of temperature-induced changes in the rates of channel closing.[51] In the case of eTLE at 50 °C with 500 nM Alm, very quick bursts in current are observed when the voltage is increased to 125 mV. Current through the same bilayer shows no channel activity at an applied voltage of 85 mV (i.e., the voltage used to elicit channel activity at 25 °C). The lifetime of a given burst at 125 mV is significantly shorter than gating events in eTLE at room temperature or even in DPhPC at 50 °C. As voltage is increased above 125 mV, the bursts become more frequent. The dynamic change in channel gating during heating is displayed in full in Figure S12 in the SI. The nature of the heated-state activity is similar for a higher peptide concentration of 5 μM with eTLE DIBs held at 50 °C. Like at 25 °C, we again observe a reduction in both the voltage required to elicit Alm-associated currents (65 mV as opposed to 125 mV with 500 nM Alm) as well as the lifetime of Alm associated gating events.

The voltage-dependent insertion of alamethicin is confirmed and characterized further versus lipid type and temperature using CV measurements. For a lipid bilayer in the presence of Alm, macroscopic conductance (and thus current) is known to increase exponentially as a function of voltage above a critical voltage threshold (V^*). Figure 9A shows representative current−voltage sweeps for eTLE and DIB DIBs containing 1μM Alm in the aqueous lipid solution at 25, 37, and 50 °C. For both membrane compositions and at all temperatures, the data show the expected exponential current response (confirmed via plotting in SI, Figure S13), a result that further validates Alm insertion in bilayers of both lipid types. V^* is determined as the voltage at which conductance exceeds a threshold conductance, G^*_{thresh}, of 8 μS/cm^2 (see SI Figure S3

DOI: 10.1021/la503471m
Langmuir 2015, 31, 325−337

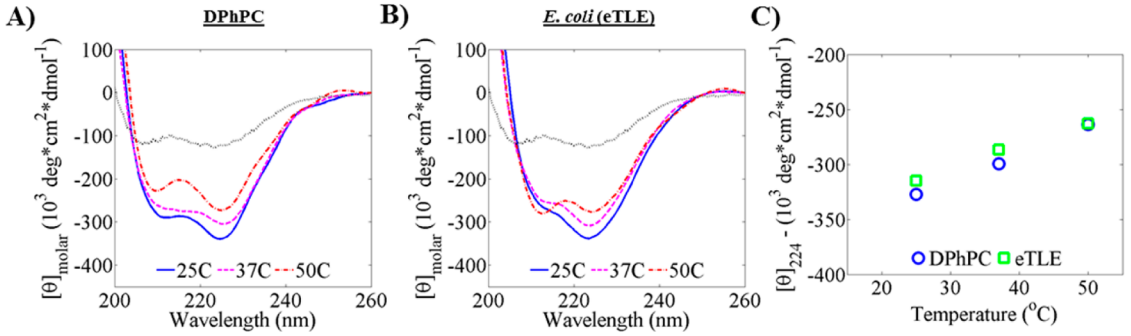

Figure 10. Molar ellipticity of alamethicin incubated with DPhpC (A) and eTLE (B) liposomes at a peptide/lipid ratio of 1:46. Samples are tested initially at 25 °C. The light dashed line shows molar ellipticity of pure Alm in aqueous buffer solution at 25 °C. Temperature is increased to 37 and 50 °C after 10 min of equilibration before each measurement. Total lipid and Alm concentrations are 500 and 50 μg/mL, respectively. (C) Molar ellipticity at 224 nm for both DPhPC and eTLE as a function of temperature.

for V^* calculation details). At each temperature tested, V^* is higher for alamethicin in DPhPC membranes than in eTLE membranes. For example, 1 μM Alm exhibits voltage thresholds of 58 and 122 mV at 25 and 50 °C, respectively, in eTLE, while the same concentration of peptide requires voltages of 130 and 145 mV, respectively, to reach the conductance threshold in DPhPC. Combining these data with the single channel observations, we conclude that Alm inserts into eTLE bilayers at lower voltages than DPhPC bilayers within the range tested of 25−50 °C. The CV data also show clearly that V^* increases with increasing temperature in both membranes. This trend is reflected by the rightward shifts in the representative exponential current traces as shown in Figure 9A, and also in the calculated values of V^* and ΔV^* (change in V^* relative to RT for each lipid) summarized in Figure 9B,C. Plotting the voltage threshold versus temperature for the two membranes (Figure 9B) reveals that V^* for alamethicin insertion in eTLE bilayers is more sensitive to temperature increases compared to insertion in DPhPC bilayers. This result is in direct agreement with the single-channel gating that was shown to occur at significantly lower voltages in eTLE membranes at 25 °C versus 50 °C.

The effects of temperature and lipid type on peptide insertion are examined quantitatively by computing other macroscopic Alm conductance parameters. V^* follows an experimental relation to the aqueous alamethicin concentration (C_a) as follows:[52,54,55]

$$V^* = -V_a \ln(C_a/C_0) \quad (1)$$

Here, V_a describes the shift in V^* (and thus the current-voltage curve) that results from an e-fold increase in C_a. Physically, V_a provides a measure of the sensitivity of membrane conductance to Alm concentration and is known to change with lipid type and temperature.[54] C_0 is a constant, representing the concentration at which Alm inserts spontaneously into the bilayer without an applied voltage. Figure 9D shows the current−voltage curves of eTLE bilayers tested at 50 °C with alamethicin concentrations ranging from 0.75-5 μM, and it is clear that the curves shift toward lower voltage (left) as peptide concentration increases. Figure 9E is a plot of $\ln(C_a)$ versus V^* obtained from data in Figure 9D (eTLE at 50 °C) as well as eTLE and DPhPC at 25 °C. Similar measurements on the effect of Alm concentration in DPhPC are not performed at 50 °C, although little change is expected due to the reduced sensitivity of V^* to temperature. Rearranging eq 1 yields $\ln(C_a) = -(1/V_a)V^* + \ln(C_0)$. Via this relation, the slope and intercept of a linear fit of the series in Figure 9E provide access to V_a and C_0 for each lipid and temperature (Figure 9F). At 25 °C, V_a is 32 mV for DPhPC and 27 mV for eTLE. Upon heating eTLE through T_g to 50 °C, V_a increases significantly to almost 60 mV, indicating that heating results in a considerable change to the membrane environment that reduces its susceptibility to Alm insertion at a given concentration. The near doubling of V_a from 25 to 50 °C provides additional support that the gel−fluid phase transition in eTLE bilayers is the cause for reduced alamethicin activity in the heated state. Further, higher values of C_0 for DPhPC versus eTLE and for eTLE at 50 °C versus 25 °C indicate that a higher concentration of Alm is required to promote insertion without applied voltage in DPhPC bilayers and heated eTLE bilayers. These results allow us to conclude that Alm inserts into eTLE membranes below its T_g at lower voltages and concentrations compared to both DPhPC bilayers at the same temperature and fluid-phase eTLE DIBs (above T_g).

CD experiments at 28, 37, and 50 °C also provide structural evidence that alamethicin insertion into lipid bilayers decreases with increasing temperature. The spectra obtained for Alm bound to eTLE and DPhPC liposomes are converted to molar ellipticity and shown in Figure 10A and B, respectively. Figure 10C shows the molar ellipticity at 224 nm, a wavelength associated with alpha-helical conformation,[55] as a function of lipid type and temperature. For both lipid types, the magnitude of ellipticity decreases with increasing temperature, which suggests decreasing alpha helical content upon heating. The alpha helical content is believed to correlate to the amount of inserted, transmembrane spanning alamethicin.[55] Thus, it appears here that the amount of inserted Alm is inversely related to the temperature. This result holds for both eTLE and DPhPC bilayers, is consistent with previous research into effects of temperature on secondary structure,[56] and is also in line with finding that V^* increases with temperature for DIBs of both lipid types.

Discussion of Alm Insertion into eTLE Membranes. There are several possible reasons as to why eTLE DIBs exposed to Alm exhibit lower voltage thresholds compared to DPhPC. Without the bulky isoprenoid methyl groups present in DPhPC,[57] an eTLE bilayer may exhibit higher fluidity and present a lower barrier to entry for Alm insertion. Phase separation and the presence of subdomains within an eTLE[58,59] may laterally concentrate regions of Alm, thereby increasing the probability of channel formation in concentrated regions. Additionally, alamethicin may itself induce local melting in the

DOI: 10.1021/la503471m
Langmuir 2015, 31, 325−337

membrane that leads to peptide-rich fluid regions even below the effective T_g for the membrane.[41] While the specifics of this mechanism are unclear from our data alone, the measurements provide strong evidence that eTLE membranes allow for Alm channel formation to occur at lower voltage and lower concentration compared to DPhPC bilayers.

Aside from differences in composition, the increases in voltage threshold (CD) and decreases in alpha-helical content (CV) suggest that the likelihood of Alm insertion decreases upon heating. The trend is consistent for both DPhPC and eTLE, however alamethicin insertion in eTLE exhibits a greater sensitivity to increases in temperature, as indicated by the larger change in voltage threshold (Figure 9A–C) and the more drastic changes to single channel currents (Figure 8B). These data suggest that the gel-to-liquid phase transition of eTLE versus heating of DPhPC within the liquid phase is the cause for the difference in temperature sensitivity for alamethicin peptide insertion between the two membranes. The results obtained from CD testing show less of a difference, however these tests were performed at much higher alamethicin concentrations required to induce spontaneous insertion without voltage. At such a high concentration needed for CD measurements, the additional peptide may have also reduced the membrane phase transition below room temperature. An increase in alamethicin activity below T_g in a mixed-lipid membrane is supported by a prior study by Boheim, et al.[41] that showed increased conductance (at a fixed voltage) upon cooling into the gel state of a binary phospholipid mixture. The authors of that work hypothesized that peptide does not prefer to insert into a gel-phase membrane, rather that cooling below the phase transition creates phase-separate subdomains in the bilayer that effectively increase the concentration of alamethicin in the fluid portions of the bilayer.[41] Our results with heterogeneous eTLE DIBs show a similar trend, and we too believe that the phase transition may drive an increase in local concentration of peptides in the membrane, which agrees with the trend for single channel lifetimes (Figure 8A and B) and voltage threshold versus alamethicin concentration (Figure 9C).

It is important, too, to put the observed temperature sensitivity of Alm insertion in context to the fact that heating *solvent-containing* DIBs results in an increased amount of oil in the membrane. The comparable magnitudes of solvent-associated changes in C_M and d_M (Figure 5) suggest eTLE and DPhPC bilayers undergo similar increases in thickness upon heating. Thus, it seems unlikely that thickness or temperature-dependent solubility of oil in the membranes are solely responsible for the changes in V^*, which were shown to be significantly larger for eTLE membranes. To help eliminate oil as the cause of the significant changes to V^* with eTLE as a function of temperature, we performed separate CV measurements on eTLE DIBs in squalene instead of hexadecane (SI, Figure S14). This substitution was made since it is known that larger-molecule oils are known to yield more *solvent-free* bilayers.[60] In the presence of squalene, V^* for an Alm concentration of 2 μM shifts from 86.2 mV at 25 °C to 49.0 mV at 50 °C after heating the bilayer from the gel phase to the fluid phase. Thus, while oil in the membrane may affect the thickness of the bilayer, and can depress the transition temperature (believed to be less than 10 °C),[61] we conclude that the effective phase change of the eTLE membrane is the dominant cause for the changes in alamethicin insertion upon heating.

CONCLUSIONS

DIB formation using total lipid extract from Gram-negative *E. coli* is enabled by heating droplets containing eTLE liposomes to 50 °C to promote monolayer formation at the oil-water interface. Through parallel measurements, we found that this temperature corresponds to the upper limit of a gel-to-liquid phase transition for the mixed liposomes. Nonetheless, bacterial model membranes comprised of eTLE lipids can be formed at cooler temperatures too, so long as heating is used to first promote adequate monolayer formation. These findings suggest that the formation of DIBs using liposomes with gel-to-liquid transition temperatures above room temperature can be performed in either the gel or liquid phase by using heat to first aid in monolayer assembly. Electrical measurements of specific capacitance confirm that like DPhPC, the interface between droplets containing eLTE liposomes is that of a lipid bilayer. Hydrophobic thicknesses for both are comparable (~26–31 Å), although the bacterial variant exhibits slightly thicker interfaces than its DPhPC counterpart. Electrical measurements reveal that eTLE DIBs are comparable to those formed using DPhPC at both room temperature and 50 °C in terms of resistance, specific resistance, and rupture potential. Plus, DIBs composed of either DPhPC or eTLE exhibit low leakage currents under applied voltage, making them suitable for electrical measurements of single or few ion channels as well as higher peptide concentrations. With the capability to vary temperature, we demonstrated that the electrical resistance and rupture potential of DPhPC and eTLE DIBs both decrease with increasing temperature. However, mixed-lipid compositions of eTLE enable reversible cycling through T_g without leakage or rupture, unlike single and binary lipid compositions that often coalesce during the transition. Specific capacitance of membranes from either lipid type decreases with increasing temperature, indicating a slight increase in thickness, which is attributed to a temperature-dependent increase in hexadecane solubility in the bilayer.

In the second part of the work, the ability to construct DIBs from *E. coli* total lipid extract enabled study of alamethicin interactions with bilayers possessing natural and heterogeneous lipid composition. The ability to control temperature allowed investigation of the role of gel–fluid phase transitions in peptide–membrane interactions. Alm inserts at lower concentrations and voltages in eTLE, likely the result of increased membrane fluidity compared to ordered structure of gel-phase DPhPC membranes. We also determined that the phase change exhibited by eTLE is a dominant cause for the greater temperature sensitivity of eTLE bilayers to alamethicin insertion. Our results show that upon cooling through T_g, the voltage required to induce channel formation drops by more than a factor of 2 (compared to a ~10% decrease in voltage threshold for DPhPC). An increase in alamethicin activity in the effective gel-phase for eTLE bilayers is thought to occur due to localized phase separation that concentrates alamethicin within the remaining fluid regions of the bilayer, leading to lower voltage threshold and longer single channel lifetimes. The temperature-dependent transition and resulting phase separation is a result of the complexity and heterogeneity of the natural total lipid extract. The output of this work advances DIB technology by providing methods to fabricate better biomimetic model membranes that could be used to study other antimicrobial peptides and many other membrane mediated processes. Given that eukaryotic TLEs are

DOI: 10.1021/la503471m
Langmuir 2015, 31, 325–337

commercially available (i.e., yeast, heart, brain, and liver), the lessons learned here may also enable rapid advances in assembling natural, biologically relevant model membranes to benefit human medical technology.

■ ASSOCIATED CONTENT

Supporting Information

Review of lipid selection and composition in prior DIB research. Experimental method details including bilayer electrical property measurements, DC step/CV waveforms, threshold voltage (V^*) calculation, and specific capacitance measurements. Current measurements during trials to demonstrate that heating promotes monolayer and DIB formation using eTLE and DPPC liposomes. Current−voltage curves for resistance calculations. Trials with cooling and heating of eTLE and DPhPC DIBs. Data to support Alm studies, including eTLE baseline current, dynamic changes in gating activity during heating, the relation between bilayer G^* and applied V, and CV with solvent-free eTLE DIBs in squalene. Summary table of calculated values for bar graphs in the manuscript. This material is available free of charge via the Internet at http://pubs.acs.org.

■ AUTHOR INFORMATION

Corresponding Author

*E-mail: ssarles@utk.edu.

Notes

The authors declare no competing financial interest.

■ ACKNOWLEDGMENTS

The authors acknowledge financial support from the Science Alliance Joint Directed Research and Development (JDRD) program and the Air Force Office of Scientific Research, Basic Research Initiative Grant Number FA9550-12-1-0464.

■ ABBREVIATIONS

Alm, alamethicin; A_M, bilayer area; CD, circular dichroism; CFA, cyclopropane fatty acid; CL, cardiolipin; C_M, specific capacitance; C_T, total bilayer capacitance; CV, cyclic voltammetry; d_M, hydrophobic thickness; DIB, droplet interface bilayer; DMPC, dimyristoylphosphatidylcholine; DPhPC, diphytanoylphosphatidylcholine; DPPC, dipalmitoylphosphatidylcholine; DSC, differential scanning calorimetry; eTLE, *E. coli* total lipid extract; GPCR, G protein-coupled receptor; RAM, regulated attachment method; RT, room temperature; SFA, saturated fatty acid; SI, Supporting Information; TC, thermocouple; T_g, gel-to-liquid transition temperature; TM, transmembrane; t_m, monolayer formation time; UFA, monounsaturated fatty acid; V^*, voltage threshold; ΔV^*, change in voltage threshold

■ REFERENCES

(1) Bayley, H.; Cronin, B.; Heron, A.; Holden, M. A.; Hwang, W. L.; Syeda, R.; Thompson, J.; Wallace, M. Droplet Interface Bilayers. *Mol. BioSyst.* **2008**, *4*, 1191−1208.

(2) Poulos, J.; Portonovo, S.; Bang, H.; Schmidt, J. Automatable Lipid Bilayer Formation and Ion Channel Measurement Using Sessile Droplets. *J. Phys.: Condens. Matter* **2010**, *22*, 454105.

(3) Funakoshi, K.; Suzuki, H.; Takeuchi, S. Lipid Bilayer Formation by Contacting Monolayers in a Microfluidic Device for Membrane Protein analysis. *Anal. Chem.* **2006**, *78*, 8169−8174.

(4) Leptihn, S.; Thompson, J. R.; Ellory, J. C.; Tucker, S. J.; Wallace, M. I. In Vitro Reconstitution of Eukaryotic Ion Channels Using Droplet Interface Bilayers. *J. Am. Chem. Soc.* **2011**, *133*, 9370−9375.

(5) Heron, A. J.; Thompson, J. R.; Mason, A. E.; Wallace, M. I. Direct Detection of Membrane Channels from Gels Using Water-in-Oil Droplet Bilayers. *J. Am. Chem. Soc.* **2007**, *129*, 16042−16047.

(6) Hwang, W. L.; Chen, M.; Cronin, B. d.; Holden, M. A.; Bayley, H. Asymmetric Droplet Interface Bilayers. *J. Am. Chem. Soc.* **2008**, *130*, 5878−5879.

(7) Sarles, S. A.; Leo, D. J. Regulated Attachment Method for Reconstituting Lipid Bilayers of Prescribed Size within Flexible Substrates. *Anal. Chem.* **2010**, *82*, 959−966.

(8) Fischer, A.; Holden, M. A.; Pentelute, B. L.; Collier, R. J. Ultrasensitive Detection of Protein Translocated through Toxin Pores in Droplet-Interface Bilayers. *Proc. Natl. Acad. Sci. U. S. A.* **2011**, *108*, 16577−16581.

(9) Syeda, R.; Holden, M. A.; Hwang, W. L.; Bayley, H. Screening Blockers Against a Potassium Channel with a Droplet Interface Bilayer Array. *J. Am. Chem. Soc.* **2008**, *130*, 15543−15548.

(10) Sarles, S. A.; Leo, D. J. Physical Encapsulation of Droplet Interface Bilayers for Durable, Portable Biomolecular Networks. *Lab Chip* **2010**, *10*, 710−717.

(11) Heron, A. J.; Thompson, J. R.; Cronin, B.; Bayley, H.; Wallace, M. I. Simultaneous Measurement of Ionic Current and Fluorescence from Single Protein Pores. *J. Am. Chem. Soc.* **2009**, *131*, 1652−1653.

(12) Tsuji, Y.; Kawano, R.; Osaki, T.; Kamiya, K.; Miki, N.; Takeuchi, S. Droplet-Based Lipid Bilayer System Integrated with Microfluidic Channels for Solution Exchange. *Lab Chip* **2013**, *13*, 1476−1481.

(13) Bogdanov, M.; Heacock, P.; Guan, Z.; Dowhan, W. Plasticity of Lipid-Protein Interactions in the Function and Topogenesis of the Membrane Protein Lactose Permease from *Escherichia coli*. *Proc. Natl. Acad. Sci. U. S. A.* **2010**, *107*, 15057−15062.

(14) Wang, X.; Bogdanov, M.; Dowhan, W. Topology of Polytopic Membrane Protein Subdomains Is Dictated by Membrane Phospholipid Composition. *EMBO J.* **2002**, *21*, 5673−5681.

(15) Zhang, W.; Campbell, H. A.; King, S. C.; Dowhan, W. Phospholipids as Determinants of Membrane Protein Topology: Phosphatidylethanolamine is Required for the Proper Topological Organization of the γ-Aminobutyric Acid Permeae (GabP) of Escherichia coli. *J. Biol. Chem.* **2005**, *280*, 26032−26038.

(16) Mansilla, M. C.; Cybulski, L. E.; Albanesi, D.; de Mendoza, D. Control of Membrane Lipid Fluidity by Molecular Thermosensors. *J. Bacteriol.* **2004**, *186*, 6681−6688.

(17) Mykytczuk, N. C.; Trevors, J. T.; Twine, S. M.; Ferroni, G. D.; Leduc, L. G. Membrane Fluidity and Fatty Acid Comparisons in Psychrotrophic and Mesophilic Strains of Acidithiobacillus Ferrooxidans under Cold Growth Temperatures. *Arch. Microbiol.* **2010**, *192*, 1005−1018.

(18) Morein, S.; Andersson, A.-S.; Rilfors, L.; Lindblom, G. Wild-Type *Escherichia coli* Cells Regulate the Membrane Lipid Composition in a Window between Gel and Non-Lamellar Structures. *J. Biol. Chem.* **1996**, *271*, 6801−6809.

(19) Mehla, J.; Sood, S. K. Substantiation in *Enterococcus faecalis* of Dose-Dependent Resistance and Cross-Resistance to Pore-Forming Antimicrobial Peptides by Use of a Polydiacetylene-Based Colorimetric Assay. *Appl. Environ. Microbiol.* **2011**, *77*, 786−793.

(20) Gether, U. Uncovering Molecular Mechanisms Involved in Activation of G Protein-Coupled Receptors. *Endocr. Rev.* **2000**, *21*, 90−113.

(21) Becker, O. M.; Marantz, Y.; Shacham, S.; Inbal, B.; Heifetz, A.; Kalid, O.; Bar-Haim, S.; Warshaviak, D.; Fichman, M.; Noiman, S. G Protein-Coupled Receptors: In Silico Drug Discovery in 3D. *Proc. Natl. Acad. Sci. U. S. A.* **2004**, *101*, 11304−11309.

(22) Farquhar, M. Multiple Pathways of Exocytosis, Endocytosis, And Membrane Recycling: Validation of a Golgi Route. *Fed. Proc.* **1983**, 2407−2413.

(23) Lodish, H.; Berk, A.; Zipursky, S. L.; Matsudaira, P.; Baltimore, D.; Darnell, J. Overview of extracellular signaling. In *Molecular Cell Biology*, 4th ed.; W. H. Freeman: New York, **2000**.

DOI: 10.1021/la503471m
Langmuir 2015, 31, 325−337

(24) Guan, Z. Discovering Novel Brain Lipids by Liquid Chromatography/Tandem Mass Spectrometry. *J. Chromatogr. B* **2009**, *877*, 2814−2821.
(25) Lugtenberg, E.; Peters, R. Distribution of Lipids in Cytoplasmic and Outer Membranes of *Escherichia coli* K12. *Biochim. Biophys. Acta, Lipids Lipid Metab.* **1976**, *441*, 38−47.
(26) Cafiso, D. Alamethicin: A Peptide Model for Voltage Gating and Protein-Membrane Interactions. *Ann. Rev. Biophys. Biomol. Struct.* **1994**, *23*, 141−165.
(27) Kim, S. H.; Franses, E. I. New Protocols for Preparing Dipalmitoylphosphatidylcholine Dispersions and Controlling Surface Tension and Competitive Adsorption with Albumin at the Air/Aqueous Interface. *Colloids Surf., B* **2005**, *43*, 256−266.
(28) Kaasgaard, T.; Mouritsen, O. G.; Jørgensen, K. Freeze/Thaw Effects on Lipid-Bilayer Vesicles Investigated by Differential Scanning Calorimetry. *Biochim. Biophys. Acta, Biomembr.* **2003**, *1615*, 77−83.
(29) Gross, L. C. M.; Heron, A. J.; Baca, S. C.; Wallace, M. I. Determining Membrane Capacitance by Dynamic Control of Droplet Interface Bilayer Area. *Langmuir* **2011**, *27*, 14335−14342.
(30) Greenfield, N. J. Using Circular Dichroism Spectra to Estimate Protein Secondary Structure. *Nat. Protoc.* **2007**, *1*, 2876−2890.
(31) Wootton, L. Bacterial Physiology: Bacillus Takes the Temperature. *Nat. Rev. Microbiol.* **2010**, *8*, 680−680.
(32) Lee, S.; Kim, D. H.; Needham, D. Equilibrium and Dynamic Interfacial Tension Measurements at Microscopic Interfaces Using a Micropipet Technique. 2. Dynamics of Phospholipid Monolayer Formation and Equilibrium Tensions at the Water−Air Interface. *Langmuir* **2001**, *17*, 5544−5550.
(33) Lindsey, H.; Petersen, N. O.; Chan, S. I. Physicochemical Characterization of 1,2-Diphytanoyl-*sn*-glycero-3-phosphocholine in Model Membrane Systems. *Biochim. Biophys. Acta, Biomembr.* **1979**, *555*, 147−167.
(34) Lopes, S.; Neves, C. S.; Eaton, P.; Gameiro, P. Cardiolipin, a Key Component to Mimic the *E. coli* Bacterial Membrane in Model Systems Revealed by Dynamic Light Scattering and Steady-State Fluorescence Anisotropy. *Anal. Bioanal. Chem.* **2010**, *398*, 1357−1366.
(35) Punnamaraju, S.; You, H.; Steckl, A. J. Triggered Release of Molecules across Droplet Interface Bilayer Lipid Membranes Using Photopolymerizable Lipids. *Langmuir* **2012**, *28*, 7657−7664.
(36) Yanagisawa, M.; Yoshida, T.-a.; Furuta, M.; Nakata, S.; Tokita, M. Adhesive Force between Paired Microdroplets Coated with Lipid Monolayers. *Soft Matter* **2013**, *9*, 5891−5897.
(37) Thiam, A. R.; Bremond, N.; Bibette, J. Adhesive emulsion bilayers under an electric field: from unzipping to fusion. *Phys. Rev. Lett.* **2011**, *107*, 068301.
(38) Thiam, A. R.; Bremond, N.; Bibette, J. From Stability to Permeability of Adhesive Emulsion Bilayers. *Langmuir* **2012**, *28*, 6291−6298.
(39) Römer, W.; Steinem, C. Impedance Analysis and Single-Channel Recordings on Nano-Black Lipid Membranes Based on Porous Alumina. *Biophys. J.* **2004**, *86* (2), 955−965.
(40) Villar, G.; Heron, A. J.; Bayley, H. Formation of Droplet Networks That Function in Aqueous Environments. *Nat. Nano* **2011**, *6*, 803−808.
(41) Boheim, G.; Hanke, W.; Eibl, H. Lipid Phase Transition in Planar Bilayer Membrane and Its Effect on Carrier-and Pore-Mediated Ion Transport. *Proc. Natl. Acad. Sci. U. S. A.* **1980**, *77*, 3403−3407.
(42) Punnamaraju, S.; Steckl, A. J. Voltage Control of Droplet Interface Bilayer Lipid Membrane Dimensions. *Langmuir* **2010**, *27*, 618−626.
(43) Valincius, G.; Heinrich, F.; Budvytyte, R.; Vanderah, D. J.; McGillivray, D. J.; Sokolov, Y.; Hall, J. E.; Lösche, M. Soluble Amyloid *β*-Oligomers Affect Dielectric Membrane Properties by Bilayer Insertion and Domain Formation: Implications for Cell Toxicity. *Biophys. J.* **2008**, *95*, 4845−4861.
(44) Langford, K. W.; Penkov, B.; Derrington, I. M.; Gundlach, J. H. Unsupported Planar Lipid Membranes Formed from Mycolic Acids of Mycobacterium Tuberculosis. *J. Lipid Res.* **2011**, *52*, 272−277.
(45) Leonenko, Z. V.; Finot, E.; Ma, H.; Dahms, T. E. S.; Cramb, D. T. Investigation of Temperature-Induced Phase Transitions in DOPC and DPPC Phospholipid Bilayers Using Temperature-Controlled Scanning Force Microscopy. *Biophys. J.* **2004**, *86*, 3783−3793.
(46) Pan, J.; Tristram-Nagle, S.; Kučerka, N.; Nagle, J. F. Temperature Dependence of Structure, Bending Rigidity, And Bilayer Interactions of Dioleoylphosphatidylcholine Bilayers. *Biophys. J.* **2008**, *94*, 117−124.
(47) Kučerka, N.; Nieh, M.-P.; Katsaras, J. Fluid Phase Lipid Areas and Bilayer Thicknesses of Commonly Used Phosphatidylcholines As a Function of Temperature. *Biochim. Biophys. Acta, Biomembr.* **2011**, *1808*, 2761−2771.
(48) White, S. H. Phase Transitions in Planar Bilayer Membranes. *Biophys. J.* **1975**, *15*, 95−117.
(49) Heimburg, T. Lipid Ion Channels. *Biophys. Chem.* **2010**, *150*, 2−22.
(50) Dixit, S. S.; Kim, H.; Vasilyev, A.; Eid, A.; Faris, G. W. Light-Driven Formation and Rupture of Droplet Bilayers. *Langmuir* **2010**, *26*, 6193−6200.
(51) Gordon, L. G. M.; Haydon, D. A. Kinetics and Stability of Alamethicin Conducting Channels in Lipid Bilayers. *Biochim. Biophys. Acta, Biomembr.* **1976**, *436*, 541−556.
(52) Eisenberg, M.; Hall, J.; Mead, C. A. the Nature of the Voltage-Dependent Conductance Induced by Alamethicin in Black Lipid Membranes. *J. Membr. Biol.* **1973**, *14*, 143−176.
(53) Sakmann, B.; Boheim, G. Alamethicin-Induced Single Channel Conductance Fluctuations in Biological Membranes. *Nature* **1979**, *282*, 336−339.
(54) Boheim, G.; Kolb, H.-A. Analysis of the Multi-Pore System of Alamethicin in a Lipid Membrane. *J. Membr. Biol.* **1978**, *38*, 99−150.
(55) Stankowski, S.; Schwarz, U. D.; Schwarz, G. Voltage-Dependent Pore Activity of the Peptide Alamethicin Correlated with Incorporation in the Membrane: Salt and Cholesterol Effects. *Biochim. Biophys. Acta, Biomembr.* **1988**, *941*, 11−18.
(56) Rizzo, V.; Stankowski, S.; Schwarz, G. Alamethicin Incorporation in Lipid Bilayers: A Thermodynamic Study. *Biochemistry* **1987**, *26*, 2751−2759.
(57) Baba, T.; Toshima, Y.; Minamikawa, H.; Hato, M.; Suzuki, K.; Kamo, N. Formation and Characterization of Planar Lipid Bilayer Membranes from Synthetic Phytanyl-Chained Glycolipids. *Biochim. Biophys. Acta, Biomembr.* **1999**, *1421*, 91−102.
(58) Doménech, Ò.; Merino-Montero, S.; Montero, M. T.; Hernández-Borrell, J. Surface Planar Bilayers of Phospholipids Used in Protein Membrane Reconstitution: An Atomic Force Microscopy Study. *Colloids Surf., B* **2006**, *47*, 102−106.
(59) Molle, G.; Dugas, J.-Y.; Duclohier, H.; Spach, G. Conductance Properties of des-Aib-Leu-des-Pheol-Phe-alamethicin in Planar Lipid Bilayers. *Biochim. Biophys. Acta, Biomembr.* **1988**, *938*, 310−314.
(60) Needham, D.; Haydon, D. A. Tensions and Free Energies of Formation of "Solventless" Lipid Bilayers. Measurement of High Contact Angles. *Biophys. J.* **1983**, *41*, 251−257.
(61) Antonov, V.; Anosov, A.; Norik, V.; Korepanova, E.; Smirnova, E. Electrical Capacitance of Lipid Bilayer Membranes of Hydrogenated Egg Lecithin at the Temperature Phase Transition. *Eur. Biophys. J.* **2003**, *32*, 55−59.

DOI: 10.1021/la503471m
Langmuir 2015, 31, 325−337